
Minimization of Circulating Currents in Parallel DC-DC Boost Converter Using Non-Linear Droop Control for Battery Energy Storage System

B. C. Chakrapani¹, C. R. Arunkumar^{1,*}, Punna Srinivas²
and Udaya Bhasker Manthati¹

¹*Electrical Engineering Department, National Institute of Technology Warangal, Telangana-506004, India*

²*Electrical Engineering Department, BVRIT HYDERABAD College Engineering for Women, Hyderabad, Telangana-500090, India*

E-mail: chakrapani95@gmail.com; acr_research@student.nitw.ac.in; srinivas.p@bvrthyderabad.edu.in; ub@nitw.ac.in

**Corresponding Author*

Received 15 July 2021; Accepted 01 December 2021;
Publication 18 February 2022

Abstract

Battery is considered the most dominant energy storage device for renewable energy-based DC microgrid systems (RE-DCMG) because of its ability to store energy for a longer duration. Here the power electronic converter plays a vital role, which acts as a bridge between the energy storage system and DC microgrid. One of the main reasons for the failure of battery systems due to the failure of the power electronic converters. To improve the redundancy and converter failure issues of battery energy storage systems (BESS), parallel operation of multiple converters are required. However, the parallel operation faces an issue of voltage imbalance between the converters which gives rise to an input circulating current. To address these issues, in this paper, we propose a nonlinear droop control based parallel DC-DC boost converter for battery

Distributed Generation & Alternative Energy Journal, Vol. 37_3, 819–844.

doi: 10.13052/dgaej2156-3306.37320

© 2022 River Publishers

energy storage system. The nonlinear droop control strategy ensures the equal battery current sharing between the parallel converters and good output voltage regulation. Moreover, SOC based controller avoids over-charging and over-discharging of the battery and the parallel converters ensure the redundancy in operation. The proposed system is designed and implemented in the MATLAB/Simulink and compared with the existing linear droop control.

Keywords: Battery storage converter, non-linear droop control, circulating current minimization, and converter redundancy.

1 Introduction

The importance of renewable energy sources has increased in recent years as a result of advances in technology and research [1]. The energy is generated and stored in the battery energy storage system (BESS) by employing power electronic converters, especially in the domain of solar energy systems [2]. The energy emanated from the sun, which had to be stored in the BESS and later on we can again feed to the DC microgrid [3, 4]. Between the load and the storage, a parallel Bi-directional DC-DC converter is utilized for power conversion. We need a converter to connect solar energy to supply the loads as well as store it in the BESS. Due to the depletion of fossil fuels, the importance of renewable energy sources has grown in recent years, particularly in power generation [5] and electric vehicles [6].

The energy stored in the BESS should be utilized in hybrid electric vehicles [7, 8]. For this application, we need a converter that converts the stored energy in the BESS to drive the vehicles. So we needed a DC-DC converter to convert the energy or store it in the BESS [9, 10]. Parallel converters are employed to provide redundancy [11]. Further ensuring that the power supply for the motor driver circuit to drive the vehicle is maintained. When employing a single converter for power supply, the failure of power electronics switch leads to the failure of power delivery to loads and results in a power outage [12].

To avoid this parallel DC-DC bidirectional converter is being used. As both the converters are of the same rating, even though one converter damages the other converter will be able to supply the power to the load without any interruption and the redundancy is obtained [13–15]. Because the parallel converters will have equal loading, there will be no additional stress on the switches. In addition, the use of centralized controller for parallel converters reduces the system redundancy, reliability and increases the complexity

for multiple parallel connected DC-DC converter systems [16]. Hence in this work a decentralized droop control is implemented to control each DC-DC converter independently. The main aim of droop control is to regulate the output voltage as well as to reduce the circulating currents between the two inductors such that there won't be any short circuits between the switches [17].

In the conventional linear droop control, the circulating currents are not minimized and the output voltage is not regulated properly [18–20]. This is due to the improper voltage regulation and circulating current that exist between the two converters [21–22]. To avoid this we are using a non-linear droop control for two converters. This scheme enables the equal load sharing between the two converters and regulation of output voltage at set point [23–25].

A single converter based energy storage integrated DC microgrid systems are presented in [26–28]. If any one of the converter failure occurs in the system, then there will be a power mismatch in the supply and the load demand. Such scenarios can be avoided by paralleling of the converters. It improves the redundancy of the DC microgrid system and ensure continues power supply without any interruption. Further if the BESS is continuously charged beyond the state of charge (SOC) limit, it may reduce the life span of the BESS [29, 30]. Hence a proper control of charging and discharging of the BESS should be needed based on SOC.

This paper mainly focuses on the design of a parallel bi-directional DC-DC converter for BESS. To realize the decentralized operation and ensure the redundancy, a nonlinear droop control is designed and implemented. The system is analyzed with different source and load variations and compared with traditional linear droop control.

The proposed system configuration and designed is presented in Section-2. The control strategy in explained in Section-3. The simulation results and comparison of proposed strategy with conventional linear droop control is presented in Section-4. The paper is concluded in Section 5.

2 System Configuration and Design

In this section, we will discuss the design of the parallel-connected DC-DC boost converter with a BESS as shown in Figure 1. The parallel connected bidirectional DC-DC boost converters share the total load demand equally. The boost converters designing equation are obtained from [29], assuming that the converters are operating in continuous conduction mode.

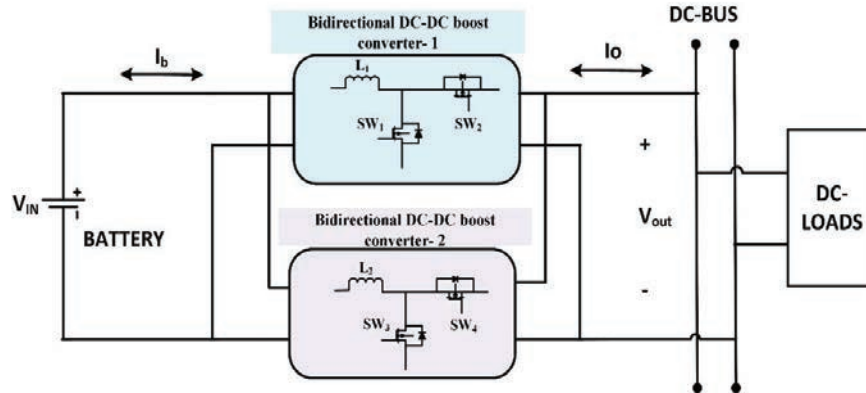


Figure 1 Block diagram of parallel-connected bi-directional DC-DC converter.

2.1 Design of Bidirectional DC-DC Converter for BESS

Figure 2 shows the parallel-connected bi-directional DC-DC converter with control strategy. Inductor value of L is used for both bi-directional DC-DC converters and are evaluated by using the following Equations (1). The non-linear droop is applied used to control the parallel converters independently. The controller values for the each control loop is tuned properly using the Single Input Single Output (SISO) tool/MATLAB [10] and the switching operation is managed based on the SOC of the BESS. The major design equations are as follows.

$$L_1 = L_2 = \frac{V_o D}{\Delta I_l f_s} \quad (1)$$

Where f_s is the switching frequency and D is the duty cycle. The L_1 and L_2 represents the input inductance of the parallel connected bi-directional DC-DC converters. Inductor ripple ΔI_l is 5%. Similarly the output capacitor of each bi-directional DC-DC converter is designed using the equation

$$C = \frac{V_o D}{\Delta V_{out} R_o f_s} \quad (2)$$

V_o and ΔV_{out} output voltage and voltage ripple in output voltage. In this analysis ΔV_{out} is 2%. The BESS system designed for handing the 144 W power and providing output voltage is 24V. Battery input voltage is taken as 24 V and output designed for 48 V. The design value is given in Table 1.

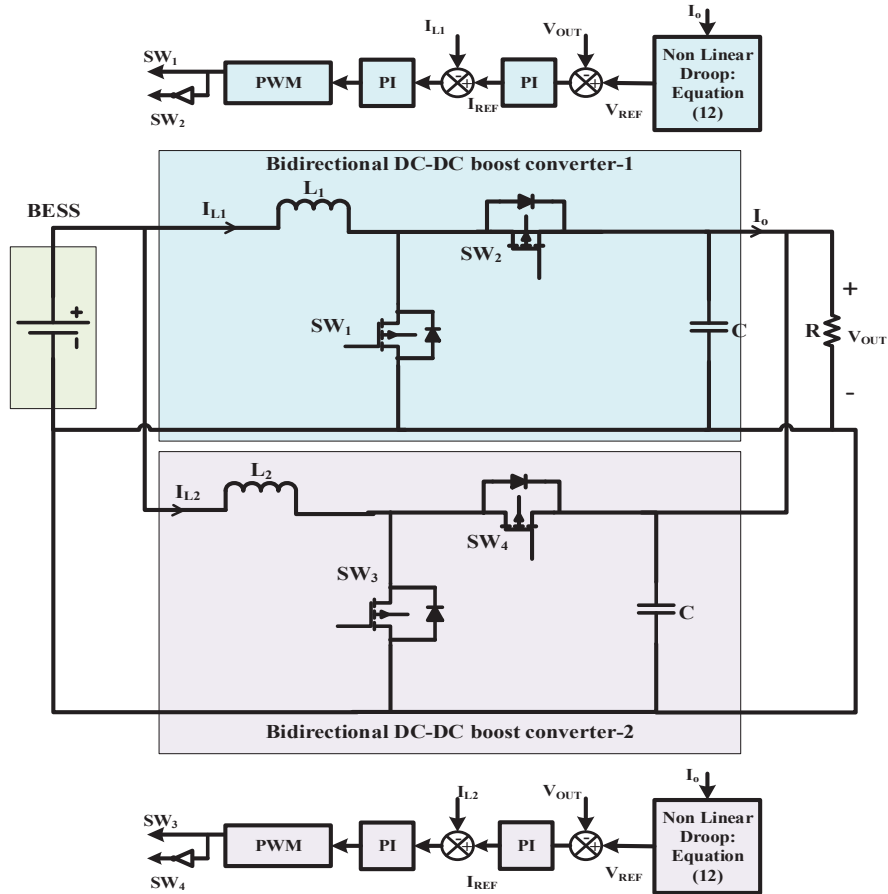


Figure 2 Circuit diagram of parallel connected bidirectional DC-DC boost converter with non-linear droop control.

2.2 Modelling of Parallel Boost Converters

Both bidirectional DC-DC boost converters are identical and operating in parallel. Hence the modelling is presented by considering single boost converter [17]. The L , C , v_c , V_0 are the filter inductor, output filter capacitance, capacitor voltage and steady state value of output voltage for boost converter respectively. The boost operation is considered for design to accommodate the effect of right hand zero in the boost converter [28]. The average equations of voltage across inductor and current through capacitor for a particular

Table 1 System parameters for simulation study

S.No	Parameters	Values
1	Battery input voltage V_{in}	12V
2	Load resistance	24 Ω
3	Boost converter inductance	2 mH
4	Output capacitance	470 μ F
5	Switching frequency	20 kHz
6	Output voltage	24 V
7	Input inductance	2 mH

switching time is given below

$$L \frac{di_l}{dt} = V_{DC} - (1 - D)V_0 \quad (3)$$

$$C \frac{dv_c}{dt} = (1 - D)i_l - \frac{v_c}{R_0} \quad (4)$$

Based on the above equations state-space equations are obtained as follows

$$\begin{bmatrix} \dot{i}_l \\ \dot{v}_c \end{bmatrix} = \begin{bmatrix} 0 & \frac{-(1-D)}{L} \\ \frac{(1-D)}{C} & \frac{-1}{R_0 C} \end{bmatrix} \begin{bmatrix} i_l \\ v_c \end{bmatrix} + \begin{bmatrix} \frac{1}{L} \\ 0 \end{bmatrix} v_{DC} \quad (5)$$

Where v_c and v_{DC} represents the instantaneous voltage across the capacitor and input voltage. V_{DC} is the BESS voltage D represents the duty cycle. The output capacitor current equation is given Equation (4).

$$\begin{bmatrix} \dot{i}_l \\ \dot{v}_c \end{bmatrix} = \begin{bmatrix} 1 & 0 \\ 0 & 1 \end{bmatrix} \begin{bmatrix} i_l \\ v_c \end{bmatrix} + DV_{DC} \quad (6)$$

The above equation are perturbed by using $v_c = V_C + \hat{v}_c$ $i_l = I_l + \hat{i}_l$, $v_{DC} = V_{DC} + \hat{v}_{DC}$ and $D = d + \hat{d}$. After doing perturbations the steady-state values to become zero because the steady-state voltage and current across the capacitor and inductor is zero, then the following equation is obtained.

$$\begin{bmatrix} \dot{\hat{i}}_l \\ \dot{\hat{v}}_c \end{bmatrix} = \begin{bmatrix} 0 & \frac{-(1-d)}{L} \\ \frac{(1-d)}{C} & \frac{-1}{R_0 C} \end{bmatrix} \begin{bmatrix} \hat{i}_l \\ \hat{v}_c \end{bmatrix} + \begin{bmatrix} \frac{V_c}{L} \\ -\frac{I_l}{C} \end{bmatrix} \hat{d} + \begin{bmatrix} \frac{1}{L} \\ 0 \end{bmatrix} \hat{v}_{DC}. \quad (7)$$

The above-average model equations are used to calculate the transfer functions for the converter.

(i) The duty cycle to the output voltage transfer function is obtained.

$$G_{\frac{v_0}{D}} = \frac{\hat{v}_0(s)}{\hat{D}(s)} = \frac{((1-d)V_0 - LI_1s)R_0}{LCR_0s^2 + Ls + (1-d)^2R_0} \quad (8)$$

(ii) The duty cycle to inductor current transfer function is derived as

$$G_{\frac{i_l}{D}} = \frac{\hat{i}_l(s)}{\hat{D}(s)} = \frac{((CV_0 + 2(1-d)I_1)R_0)}{LCR_0s^2 + Ls + (1-d)^2R_0} \quad (9)$$

(iii) The inductor current to output voltage is derived from the above Equations (8) and (9) as follows.

$$\frac{\hat{v}_0(s)}{\hat{i}_l(s)} = \frac{(1-d)V_0 - LI_1s}{CV_0s + 2(1-d)I_1} \quad (10)$$

3 Control Strategy

3.1 Design Control Strategy for BESS

The designed control strategy for the BESS is shown in Figure 3. The power-sharing between the two converters and voltage regulating is achieved by the nonlinear droop control with the help of PI controllers. $G_{\frac{i}{d}}$ is the current to duty cycle transfer function for the regulation of the current through

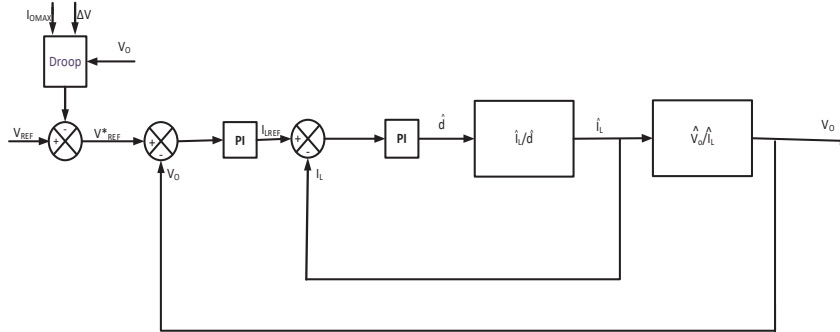


Figure 3 Controller block diagram with droop logic.

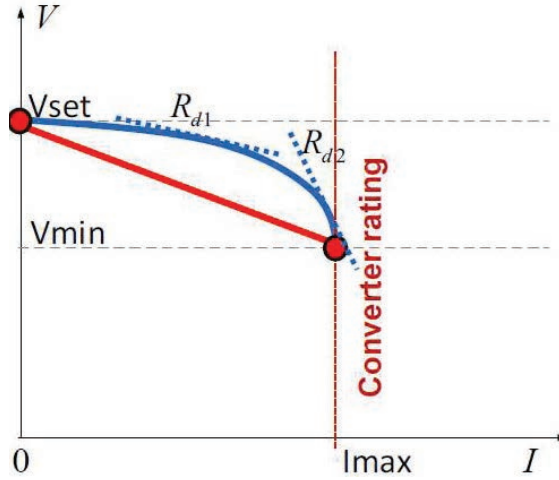


Figure 4 The linear and nonlinear droop curve.

inductors. In the design of linear droop, a linear equation is considered i.e. between the voltage and current by using the following equation [31].

$$V_{Droop} = V_{out} - I_L * R_{Droop} \quad (11)$$

V_{Droop} = droop voltage

V_{out} = output voltage

I_L = load current

R_{Droop} = droop resistance

Where R_{Droop} is calculated by the no-load voltage to I_{peak} load current.

While designing the nonlinear droop equation, we consider the inverse parabola equation for reducing the circulating currents among the converters by using the following equation [3]. The below Figure 4 explains the nonlinear droop curve. The Equation (12) represents the nonlinear droop equation based on the parabolic curve.

$$V = V_{no} - \Delta V_{out} + \left(\left(1 - \frac{i}{I_{max}} \right)^{1/2} \right) * \Delta V_{out} \quad (12)$$

Where;

ΔV_{out} = designed droop voltage range.

V_{no} = no-load voltage set point.

I_{max} = maximum output current.

In the designing of the inner current and outer current loop PI values, bandwidth plays a vital role. While tuning the PI controller bandwidth of the inner current loop is taken as 10 krad/sec to make the loop act faster compared to outer loop. The outer voltage control loop is designed with bandwidth of 600 rad/sec.

The tuning of the PI controller is based on the phase margin and gain margin concept by using the above voltage to control and current to control transfer function by solving those above two equations we will get the k_p and k_i values because the converter is identical so the same k_p and k_i values have been used to both converters.

$$P I_z = K_{zp} + \frac{K_{zi}}{s} \quad (13)$$

Where z represents the current loop and voltage loop PI values.

3.2 SOC Calculations and Application of SOC

In the switching of the converters are based on the BESS SOC and the converter will act as bi-directional DC-DC converter. When the SOC is 80% the BESS will supply the power. While the SOC is less than the 20% the BESS will be charging from the DC microgrid. The SOC calculated from the following equation [31, 32].

$$SOC(t) = SOC(t - 1) + \frac{I(t)}{Q_n} * \Delta t \quad (14)$$

Where, $SOC(t - 1)$ is the initial SOC at previous sampling, $I(t)$ is the discharging current, Q_n is the nominal capacity and Δt is the time interval. The PI values derived for the inner current control loop with the help of the SISO tool. The PI values obtained for the inner current loop is $K_{pc} = 0.134$ and $K_{ic} = 138$. The phase margin without using any compensator is -90 degree at 0 dB line while after compensating with by proper tuning the phase margin at the 0 dB line is -69 dB it indicates that the system is stable if it is operated in that prescribed limits.

The outer voltage control loop is designed for 60° phase margin and 600 rad/sec band width. The PI values obtained for inner current loop is $K_{pc} = 0.05$ and $K_{ic} = 61.125$. The phase margin without using any compensator is -94.6 degree at 0 dB line while after compensating with by proper tuning the phase margin at the 0 dB line is -59.6 dB it indicates that the system is stable if it is operated in that prescribed limits. The bode plots for

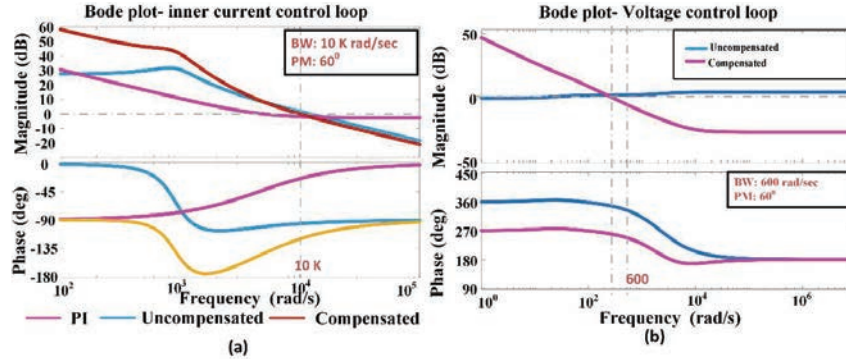


Figure 5 Bode plot (a) inner current control loop (b) outer voltage control loop.

uncompensated and compensated system is shown in Figure 5(a) and 5(b). It is clear from the bode plot that the compensated system have more gain at low frequency and less gain at high frequency.

4 Simulation Results

The linear and non-linear droop designed for parallel-connected boost converter of 144 W. The component ratings and design requirement are shown in Table 1. The system is simulated by using the MATLAB/Simulink. By giving the load variation and the source variation the performance of the controller is verified.

4.1 Linear Droop

In linear droop, the equation has been derived as mentioned above Equation (11) and it's stimulated with the help of MATLAB/Simulink. The output voltage is regulated at 24 V. The DC bus voltage, the inductor currents and circulating current waveforms are shown in Figure 6. In linear droop, the circulating current is approximately 20 mA.

4.2 Nonlinear Droop

The nonlinear droop controlled parallel bidirectional DC-DC boost converter is simulated in MATLAB/Simulink. In nonlinear droop Equation (12) is utilized to reduce the circulating current in the inductors. The proposed system is simulated for different scenarios such as load variation, source variation and compared with linear droop. The result are as follows.

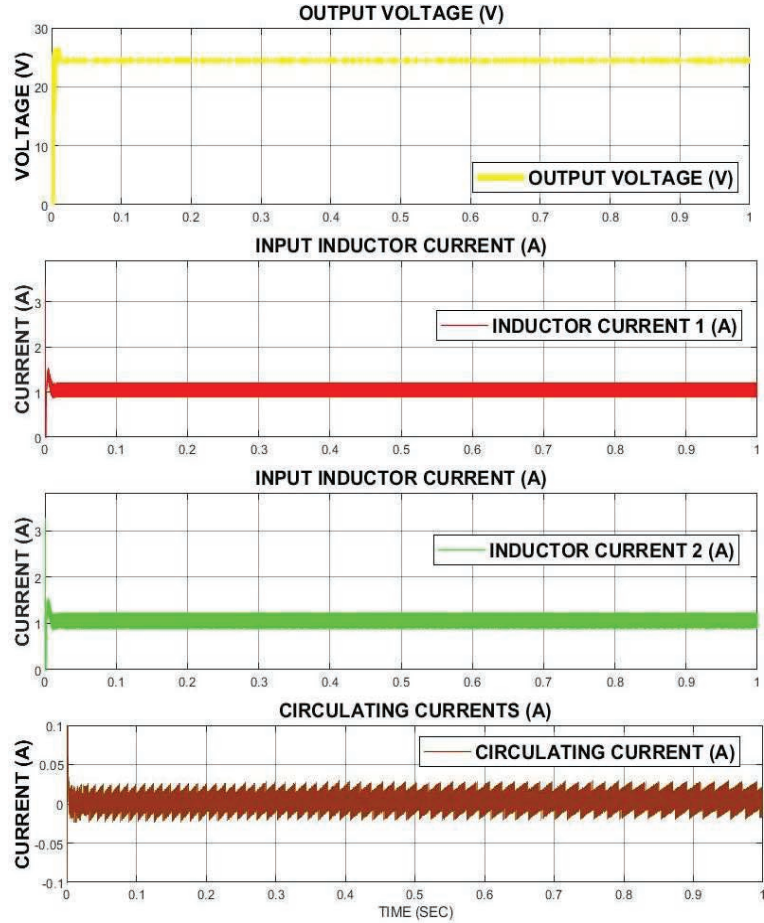


Figure 6 Simulation results for linear droop: output voltage, input inductors, circulating currents.

4.2.1 Load Disturbance

Three load variations are applied to the proposed system to verify the controller operation under load variation. The disturbance are created at 0.2 sec, 0.5 sec and 0.8 sec. The total connected load is increased at 0.2 sec and 0.5 sec and reduced at 0.8 sec. Figure 7 shows the output current through actively connected load, output voltage, BESS voltage, BESS current of the converter. At 0.2 sec load demand is increased by 25% as BESS current increasing from 8 A to 10 A. A sudden dip occur at the DC bus voltage and active load current due to increase in load demand. At, 0.8 sec, the load is suddenly disconnected.

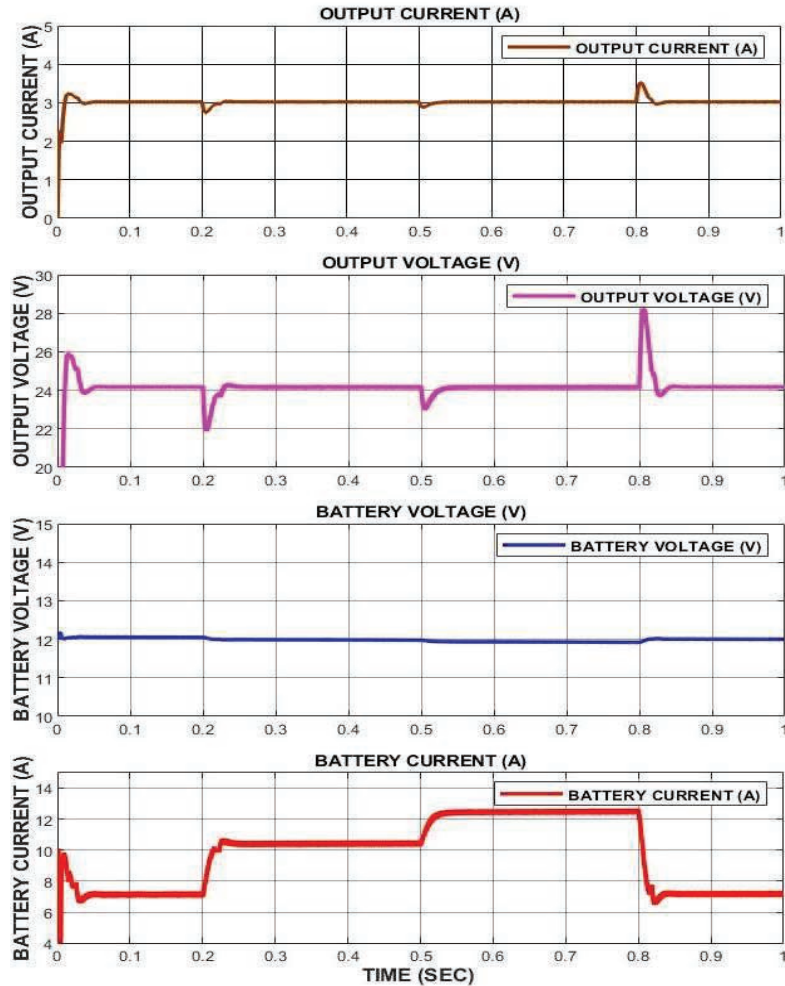


Figure 7 Simulation results for nonlinear droop under load disturbance: output current in actively connected load, output voltage, BESS voltage, BESS current.

As a result a sudden rise occur in the DC bus voltage due to the excess power exist in the load side.

Figure 8 shows the circulating current, droop voltage and BESS SOC during load disturbance. The circulating current, which is the difference between the two inductors is 2(nA), which negligible current. The difference between the two inductor is approximately zero which implies the circulating current is approximately zero. The droop voltage which is added to the

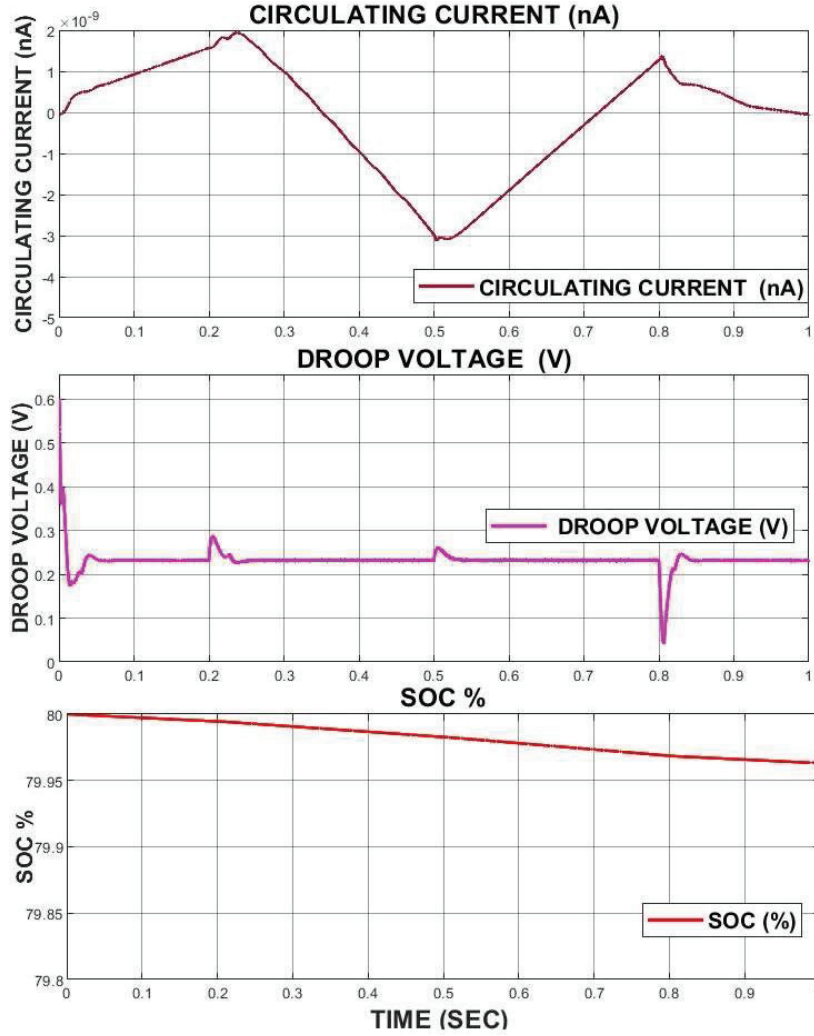


Figure 8 Simulation results for nonlinear droop under load disturbance: circulating currents, droop voltage, soc (%).

reference and feeds back to regulate the output voltage to the rated value. The SOC of the battery has linear characteristics in the operating range and falls as the BESS gets a discharged.

Figure 9 represents the inductor current of two converters and the total BESS current supplied to the converter at the time of load disturbance.

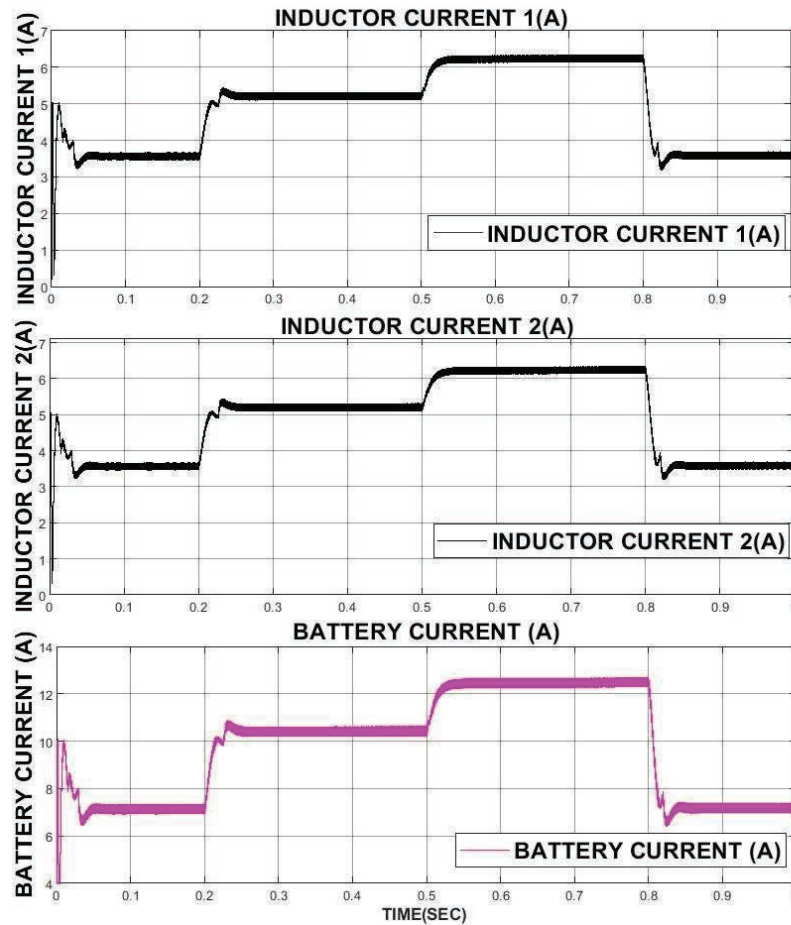


Figure 9 Simulation results for nonlinear droop under load disturbance: inductor current (1), inductor current (2), BESS current.

Initially, the total BESS current is 7 A, and the inductor currents are 3.5 A each. At the time of disturbance, the total change in load demand is shared equally between two converters. As in the Figure it is seen that the converter as supplying the equal amount to input current to satisfy the load requirement.

Figure 10 shows the power sharing in the system. The 8 ohm resistor is the active load in the system. 24 ohm and 48 ohm are connected and disconnected at different intervals. The load power demand of 8 ohm, 24 ohm and 48 ohm are 72 W, 24 W and 12 W respectively. The load power increased from 72 W to 96 W at 0.2 sec and again increased to 108 W at 0.5 sec. The

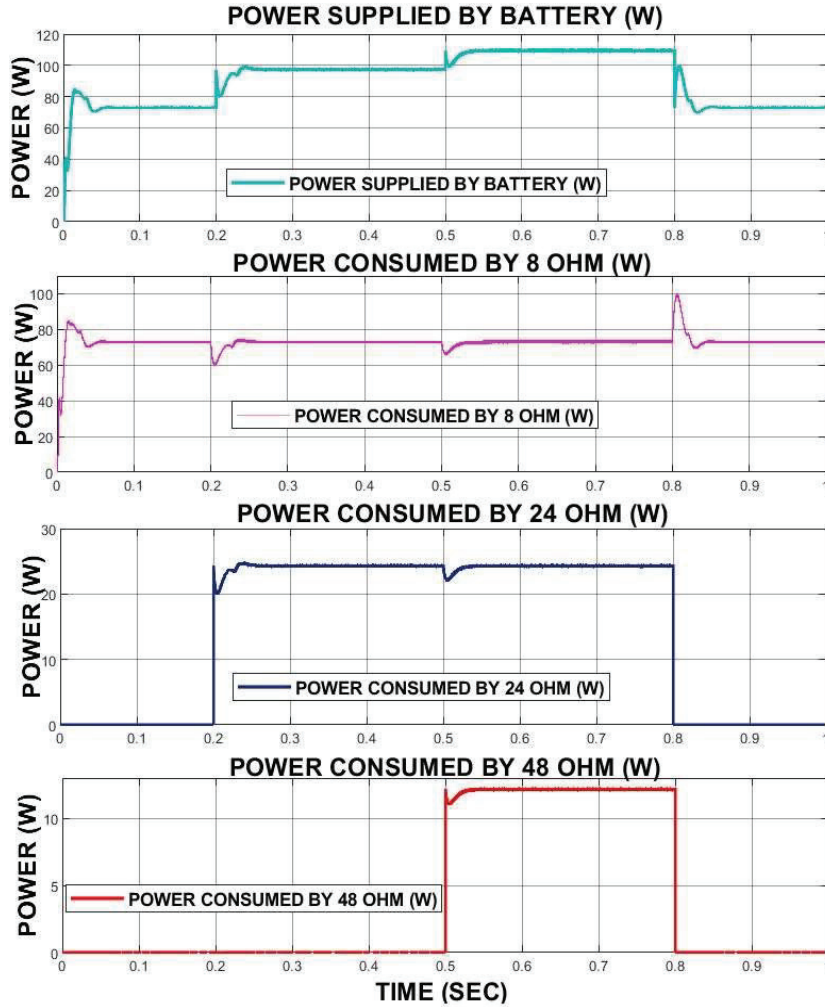


Figure 10 Simulation results for nonlinear droop under load disturbance: power supplied by BESS and power consumed by the different linear loads.

BESS supplies the total power demand. At, 0.8 sec, the power demand drops to 72 W. The power sharing of battery and connected loads reveal that the potential operation of proposed system.

In summary, the parallel connected bidirectional boost converter able to mitigate the effect of circulating current and the total load demand is shared between the two converters using proposed nonlinear droop control strategy.

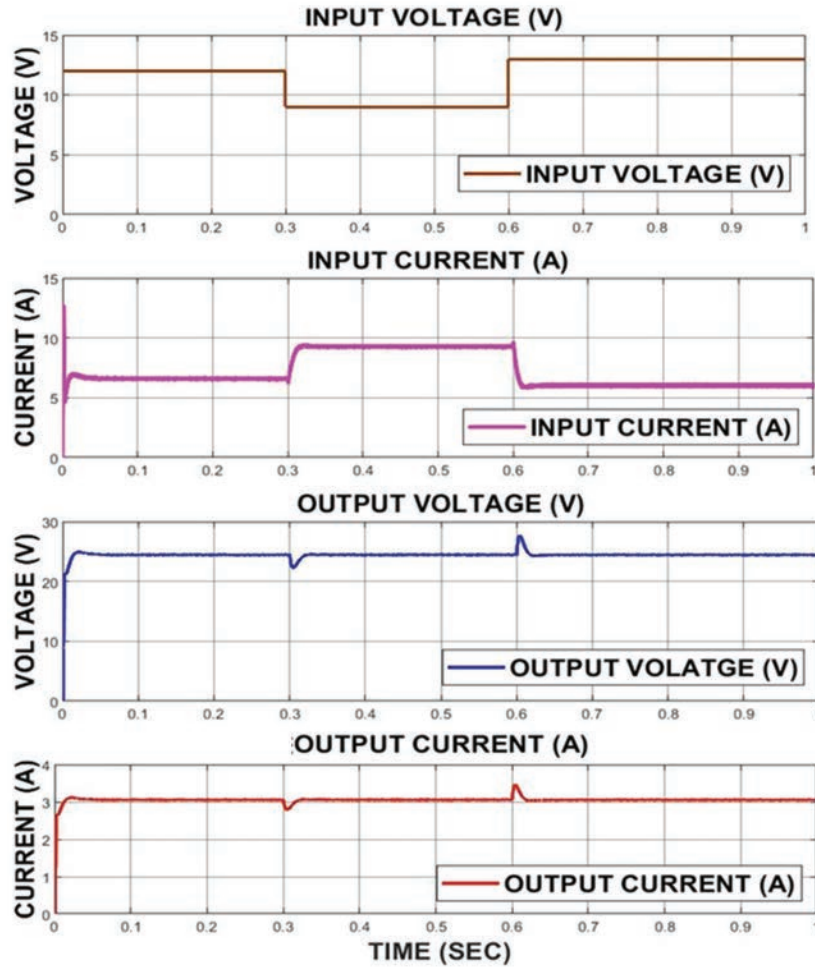


Figure 11 Simulation results for nonlinear droop under source disturbance: input voltage, input current, output voltage, and output current.

4.2.2 Source Disturbance

As source disturbance can't be created by using the BESS, a controlled DC source is connected instead of the BESS to verify the operation of the proposed controller. The disturbances are applied at 0.3 and 0.6 sec. Initially, the source voltage is 12 V, load voltage is 24 V and load current is 3 A.

At 0.3 sec, source disturbance has been introduced by reducing the value of the source voltage by 33% of the rated source voltage. Figure 12 shows the

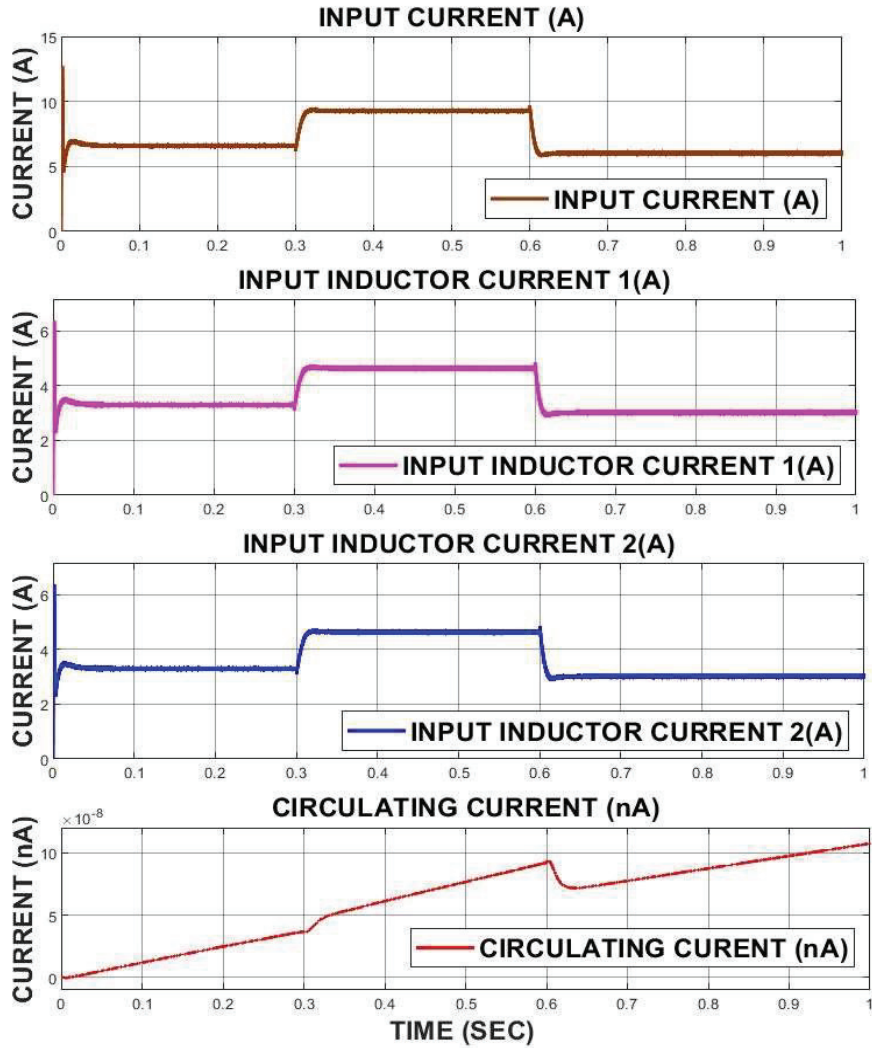


Figure 12 Simulation results for nonlinear droop under source disturbance: input inductor currents 1&2, input current, circulating current.

input voltage, input current, output voltage and output current at the time of source disturbance. The DC bus voltage is stabilized with a minor dip at the time of disturbance. The input current increased to compensate the reduction in source voltage. The load current is maintained constant at 3 A. At 0.6 sec, the source voltage is increased by 42% of rated voltage. The load is equally

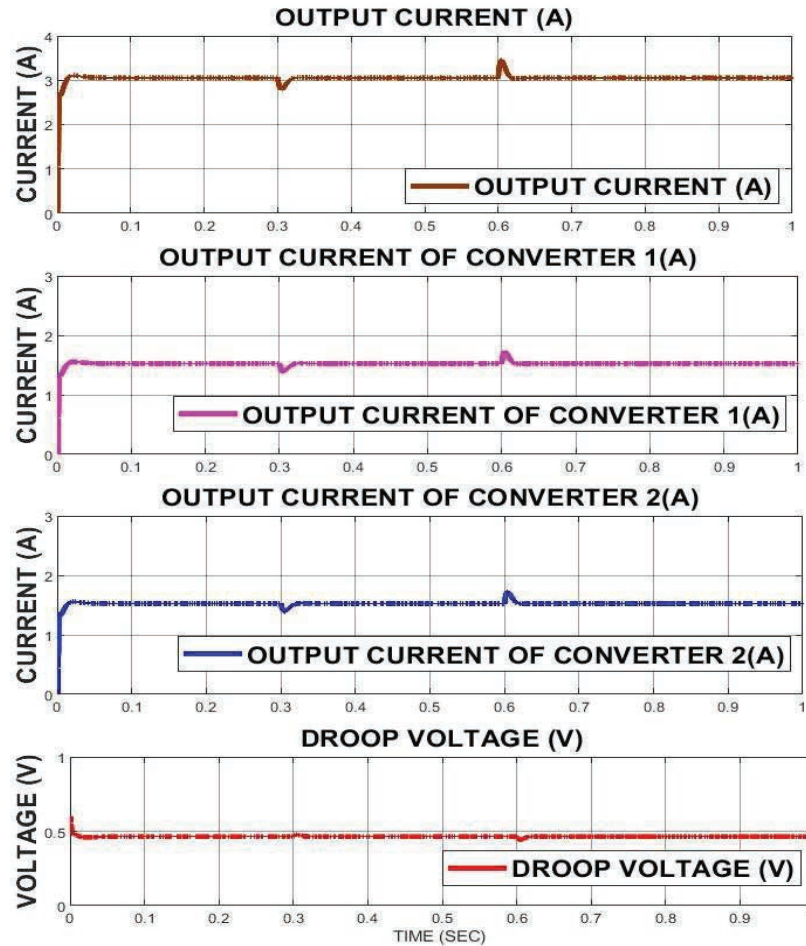


Figure 13 Simulation results for nonlinear droop under source disturbance: converter output currents, total output current, and droop voltage.

shared among the two converters by minimizing the circulating current. The source current is reduced to balance the power demand and load current is regulated at 3 A.

Figure 12 shows the total input current, two inductor currents, and circulating current, during the source disturbance. The total source current is shared between the converters equally. At the time of disturbance, the total load current is 9.6 A and is shared equally between the inductors as 4.8 A. Also, it is important to note that the circulating current is in the order on

Table 2 Comparison between linear droop and nonlinear droop

S. No	Parameters	Linear Droop	Non-Linear Droop
1	Difference between inductors	20 mA	2 nA
2	Output voltage	23 V	23.8 V

nA rating. The difference between the two inductors current is approximately zero, which implies that both the inductors are carrying the same amount of current.

Figure 13 shows the total output current, output current of two converters and the droop voltage. The total load current is 3 A. The output of each converter is 1.5 A irrespective of the source variation. The droop voltage is 0.45 V. The droop voltage is added to the reference voltage and feed to the controller to minimize the error in independent controllers. Irrespective of the operating conditions, the two converters share the power demand and load current equally.

4.3 Comparison Between Linear and Nonlinear Droop

In this section, the detailed comparison between linear and nonlinear droop is presented. While in the linear droop control, the circulating currents are not minimized below 0.02 A. As a result, a part of the battery energy is circulating in the parallel connected converter system. Further this circulating current affects the dc bus voltage regulation and leads to drop in load voltage. On the other hand, the proposed nonlinear controller for parallel connected bidirectional DC-DC boost converter reduces the circulating current and steady state error in DC bus voltage. The circulating current in nonlinear droop control is 2 nA and the steady state error in 0.2 V. A summary of the comparison is presented in Table 2. As a result, the proposed system with nonlinear droop control shows enhanced performance compared to traditional linear droop control.

5 Conclusion

In this work, a parallel bidirectional DC-DC converter is designed for BESS with redundancy and reliability in operation to regulate the output DC bus voltage. In conventional single converter based systems are lacking in redundancy and they are always subjected to high current stress. The use of parallel converter system improves the redundancy and protect the system from power outage. However, the use of centralized controller reduces the redundancy

and reliability in the system. The use of decentralized control improves the reliability, however the linear droop control lacks in DC bus voltage regulation and minimization of circulating current. This issues are addressed in this work and proposed a nonlinear droop control structure that track the set point voltage in parabolic path. The proposed system ensure equal power sharing between the converters and better DC bus voltage regulation compared to the conventional linear droop. Further, the simulation study reveals that the proposed method reduces the circulating current considerably compared to the traditional linear droop control. The SOC of the BESS is regulated with in predefined limits. The transient and steady-state ripple in the voltage and current have been in permissible limits. The redundancy is also implemented and the switching actions are done based on the SOC of the BESS, while the BESS charging and discharging have been controlled.

References

- [1] Bull SR. Renewable energy today and tomorrow. Proceedings of the IEEE. 2001 Aug;89(8):1216–26.
- [2] Punna S, Manthathi UB, Chirayarukil Raveendran A. Modeling, analysis, and design of novel control scheme for two-input bidirectional DC-DC converter for HESS in DC microgrid applications. *International Transactions on Electrical Energy Systems*. 2021 Jan 4:e12774.
- [3] Babu NP, Babu CB, Peesapati RB, Panda G. An optimal current control scheme in grid-tied hybrid energy system with active power filter for harmonic mitigation. *International Transactions on Electrical Energy Systems*. 2019 Dec 17.
- [4] Kumar GB, Palanisamy K, De Tuglie E. Energy Management of PV-Grid-Integrated Microgrid with Hybrid Energy Storage System. In 2021 IEEE International Conference on Environment and Electrical Engineering and 2021 IEEE Industrial and Commercial Power Systems Europe (EEEIC/I&CPS Europe) 2021 Sep 7 (pp. 1–6). IEEE.
- [5] Vavilapalli S, Padmanaban S, Subramaniam U, Mihet-Popa L. Power balancing control for grid energy storage system in photovoltaic applications—Real time digital simulation implementation. *Energies*. 2017 Jul;10(7):928.
- [6] Katnapally A, Manthathi UB, Chirayarukil Raveendran A, Punna S. A predictive power management scheme for hybrid energy storage system in electric vehicle. *International Journal of Circuit Theory and Applications*. 2021 Aug 20.

- [7] Deng, J., Shi, J., Liu, Y. and Tang, Y., 2016. Application of a hybrid energy storage system in the fast-charging station of electric vehicles. *IET Generation, Transmission & Distribution*, 10(4), pp. 1092–1097.
- [8] Kumar R, Padmanaban S. Electric vehicles for India: overview and challenges. *IEEE India Informatics*. 2019 Apr;14:139.
- [9] Arunkumar, C.R., Manthathi, U.B. and Punna, S., 2021. Supercapacitor-based transient power supply for DC microgrid applications. *Electrical Engineering*, pp. 1–10.
- [10] Punna, S., and Manthathi, U.B., 2020. Optimum design and analysis of a dynamic energy management scheme for HESS in renewable power generation applications. *SN Applied Sciences*, 2(3), pp. 1–13.
- [11] Mazumder SK, Tahir M, Acharya K. Master–slave current-sharing control of a parallel DC–DC converter system over an RF communication interface. *IEEE Transactions on Industrial Electronics*. 2008 Jan 4;55(1):59–66.
- [12] Thounthong P, Mungporn P, Pierfederici S, Guilbert D, Takorabet N, Nahid-Mobarakeh B, Hu Y, Bizon N, Huangfu Y, Kumam P, Burikham P. Robust Hamiltonian-Energy Control Based on Lyapunov Function for Four-Phase Parallel Fuel Cell Boost Converter for DC Microgrid Applications. *IEEE Transactions on Sustainable Energy*. 2021 Jan 12.
- [13] Wang YF, Xue LK, Wang CS, Wang P, Li W. Interleaved high-conversion-ratio bidirectional DC–DC converter for distributed energy-storage systems—circuit generation, analysis, and design. *IEEE Transactions on Power Electronics*. 2015 Nov 2;31(8):5547–61.
- [14] Mazumder, S.K., Tahir, M., and Acharya, K., 2008. Master-slave current-sharing control of a parallel DC-DC converter system over an RF communication interface. *IEEE Transactions on Industrial Electronics*, 55(1), pp. 59–66.
- [15] Augustine, S., Mishra, M.K., and Lakshminarasamma, N., 2014. Adaptive droop control strategy for load sharing and circulating current minimization in low-voltage standalone DC microgrid. *IEEE Transactions on Sustainable Energy*, 6(1), pp. 132–141.
- [16] Ashourloo M, Namburi VR, Piqué GV, Pigott J, Bergveld HJ, El Sherif A, Trescases O. Decentralized quasi-fixed-frequency control of multiphase interleaved hybrid Dickson converters for fault-tolerant automotive applications. *IEEE Transactions on Power Electronics*. 2019 Dec 9;35(7):7653–63.
- [17] Xu Q, Hu X, Wang P, Xiao J, Tu P, Wen C, Lee MY. A decentralized dynamic power sharing strategy for hybrid energy storage system in

- autonomous DC microgrid. *IEEE transactions on industrial electronics*, 2016 Sep 13;64(7):5930–41.
- [18] Khorsandi, A., Ashourloo, M., and Mokhtari, H., 2014. A decentralized control method for a low-voltage DC microgrid. *IEEE Transactions on Energy Conversion*, 29(4), pp. 793–801.
- [19] Lu, X., Guerrero, J.M., Sun, K., and Vasquez, J.C., 2013. An improved droop control method for dc microgrids based on low bandwidth communication with dc bus voltage restoration and enhanced current sharing accuracy. *IEEE Transactions on Power Electronics*, 29(4), pp. 1800–1812.
- [20] Gu, Y., Xiang, X., Li, W., and He, X., 2013. Mode-adaptive decentralized control for renewable DC microgrid with enhanced reliability and flexibility. *IEEE Transactions on Power Electronics*, 29(9), pp. 5072–5080.
- [21] Chen, F., Burgos, R., Boroyevich, D., Vasquez, J.C., and Guerrero, J.M., 2019. Investigation of nonlinear droop control in DC power distribution systems: Load sharing, voltage regulation, efficiency, and stability. *IEEE Transactions on Power Electronics*, 34(10), pp. 9404–9421.
- [22] Prabhakaran, P., Goyal, Y. and Agarwal, V., 2017. A novel communication-based average voltage regulation scheme for a droop-controlled DC microgrid. *IEEE Transactions on Smart Grid*, 10(2), pp. 1250–1258.
- [23] Du, Y., Huang, A.Q., Yu, X. and Li, J., 2013, March. Droop controller design methods for isolated DC-DC converter in DC grid battery energy storage applications. In *2013 Twenty-Eighth Annual IEEE Applied Power Electronics Conference and Exposition (APEC)* (pp. 1630–1637). IEEE.
- [24] Prabhakaran, P., Goyal, Y. and Agarwal, V., 2017. Novel nonlinear droop control techniques to overcome the load sharing and voltage regulation issues in DC microgrid. *IEEE Transactions on power electronics*, 33(5), pp. 4477–4487.
- [25] Maknouninejad, A., Qu, Z., Lewis, F.L., and Davoudi, A., 2014. Optimal, nonlinear, and distributed designs of droop controls for DC microgrids. *IEEE Transactions on Smart Grid*, 5(5), pp. 2508–2516.
- [26] Pavlovic, T., Bjazic, T., and Ban, Z., 2012. Simplified averaged models of DC-DC power converters suitable for controller design and microgrid simulation. *IEEE Transactions on Power Electronics*, 28(7), pp. 3266–3275.

- [27] Sanjeev, P., Padhy, N.P., and Agarwal, P., 2018. Autonomous power control and management between standalone DC microgrids. *IEEE Transactions on Industrial Informatics*, 14(7), pp. 2941–2950.
- [28] Arunkumar, C.R., Manthati, U.B., 2019, October. Design and Small Signal Modelling of Battery-Supercapacitor HESS for DC Microgrid. In *TENCON 2019-2019 IEEE Region 10 Conference (TENCON)* (pp. 2216–2221). IEEE.
- [29] Arunkumar CR, Manthati UB, Srinivas P. Accurate modelling and analysis of battery–supercapacitor hybrid energy storage system in DC microgrid systems. *Energy Systems*. 2021 Jul 26:1–9.
- [30] S. Anand B.G. Fernandes, “Modified droop controller for paralleling of dc-dc converters in standalone dc system modified droop controller for paralleling of dc-dc converters in standalone dc system,” *IET Power Electronics* 3rd February 2012.
- [31] Chang, W.Y., 2013. The state of charge estimating methods for battery: A review. *ISRN Applied Mathematics*, 2013.
- [32] Rosewater, D.M., Copp, D.A., Nguyen, T.A., Byrne, R.H., and Santoso, S., 2019. Battery Energy Storage Models for Optimal Control. *IEEE Access*, 7, pp. 17827–178391.

Biographies



B. C. Chakrapani received his B.Tech. degree in Electrical and Electronics Engineering from Institute of Aeronautical Engineering, Dundigal, Hyderabad, India in 2016 and Master’s in Power Electronics and Drives from National Institute of Technology-Warangal, India in 2020, respectively. His research interest are energy storage systems, power electronic converters and applications.



C. R. Arunkumar received B.Tech and M.Tech degree in Electrical and Electronics Engineering and Power Electronics and control from Mahatma Gandhi University Kottayam, Kerala in 2013 and 2016 respectively. He is presently working towards Doctoral Program from National Institute of Technology-Warangal, India. His research interests include DC microgrid, Hybrid Energy Storage systems and DC-DC converters.



Punna Srinivas received B.Tech degree in electrical and electronics engineering from JNTU, Hyderabad, India in 2006. The Masters (M.Tech) and Ph.D in Power Electronics and Drives from National Institute of Technology-Warangal, India in 2009 and 2021 respectively. Currently, he is working as Assistant Professor at BVRIT Hyderabad College of Engineering for Women, Hyderabad, India. His research interests include design and modeling of DC-DC converters for Energy storage systems, DC microgrid integrated hybrid energy storage system for linear and non-linear control technique.



Udaya Bhsaker Manthathi received B.Tech degree in electrical and electronics engineering and M.E. in Power Electronics & Drives in 2003 and 2006 and Ph.D. in electrical engineering in 2011. Since 2012, he has been working as Assistant professor in department of electrical engineering at National Institute of Technology-Warangal, India. In 2011, he worked as Assistant professor at Manipal University Jaipur-India. He was a research assistant at CITCEA-UPC, Spain during 2007–2011. His research interest include bi-directional DC-DC converters, power electronics application to micro grid and smart grid technologies, energy storage systems, digital control and synchrotrons power supplies. He is a recipient of SLL-UPC fellowship during 2007–2010.

